ADVANCING EARTH AND SPACE SCIENCE

JGR Atmospheres

RESEARCH ARTICLE

10.1029/2022JD037065

Key Points:

- Decadal relationship between the Northern Hemisphere land monsoon rainfall (NHLMR) and extended El Niño/Southern Oscillation is robust over the past millennium
- A decadal relationship between NHLMR and North Atlantic–south Indian Ocean dipole (NAID) emerged about 1700 under volcanic eruptions
- Successive northern volcanic eruptions reduce thermal contrast between the two hemispheres, causing a resonant NHLMR-NAID behavior

Supporting Information:

Supporting Information may be found in the online version of this article.

Correspondence to:

W. Sun,
weiyisun@njnu.edu.cn

Citation:

Shen, T., Sun, W., Liu, J., Wang, B., Chen, D., Ning, L., & Chen, K. (2022). Secular changes of the decadal relationship between the Northern Hemisphere land monsoon rainfall and sea surface temperature over the past millennium in climate model simulations. *Journal of Geophysical Research: Atmospheres*, *127*, e2022JD037065. https://doi.org/10.1029/2022JD037065

Received 6 MAY 2022
Accepted 25 NOV 2022
Corrected 17 JAN 2023

This article was corrected on 17 JAN 2023. See the end of the full text for details.

Author Contributions:

Conceptualization: Weiyi Sun, Jian Liu, Bin Wang, Deliang Chen
Formal analysis: Tianyin Shen, Weiyi Sun
Methodology: Tianyin Shen, Liang Ning, Kefan Chen

Secular Changes of the Decadal Relationship Between the Northern Hemisphere Land Monsoon Rainfall and Sea Surface Temperature Over the Past Millennium in Climate Model Simulations

Tianyin Shen[1], Weiyi Sun[1], Jian Liu[1,2,3], Bin Wang[4], Deliang Chen[5], Liang Ning[1], and Kefan Chen[1]

[1]Key Laboratory for Virtual Geographic Environment, Ministry of Education, State Key Laboratory Cultivation Base of Geographical Environment Evolution of Jiangsu Province, Jiangsu Center for Collaborative Innovation in Geographical Information Resource Development and Application, School of Geography Science, Nanjing Normal University, Nanjing, China, [2]Jiangsu Provincial Key Laboratory for Numerical Simulation of Large Scale Complex Systems, School of Mathematical Science, Nanjing Normal University, Nanjing, China, [3]Open Studio for the Simulation of Ocean-Climate-Isotope, Qingdao National Laboratory for Marine Science and Technology, Qingdao, China, [4]Department of Atmospheric Sciences and Atmosphere-Ocean Research Center, University of Hawaii at Manoa, Honolulu, HI, USA, [5]Regional Climate Group, Department of Earth Sciences, University of Gothenburg, Gothenburg, Sweden

Abstract Understanding the decadal variability of Northern Hemisphere land monsoon rainfall (NHLMR) is crucial to social-economic development. However, due to the temporal limitation of instrumental data, the decadal relationship between NHLMR and sea surface temperature (SST) remains uncertain. The extended El Niño–Southern Oscillation (XEN) SST index and the North Atlantic–south Indian Ocean dipole (NAID) SST index can be the predictors to help us understand the decadal relationship between NHLMR and SST. In this study, using the Community Earth System Model-Last Millennium Ensemble (CESM-LME) simulations, we find a significant and stable decadal correlation between the NHLMR and XEN in the all-forcing (AF) (with natural and anthropogenic forcings, AF), control (internal variability only), and other external forcings run over the past millennium, which means that this simulated NHLMR-XEN relationship is caused by internal variability. The AF experiments show that the decadal relationship between NHLMR and NAID is practically non-existent until an abrupt and significant increase in volcanic eruptions at about 1700, which is also indicated by the Paleoclimate Modeling Intercomparison Project Phase 3 (Paleoclimate Modeling Intercomparison Project Phase 3) simulations. Using the volcanic forcing sensitivity experiments, we find that the successive strong volcanic eruptions in the Northern Hemisphere (NH) significantly strengthen the synchronous changes of NHLMR and NAID after 1700, with a periodicity of 20–40-year for NHLMR and NAID. Specifically, successive NH eruptions weaken the north-south hemispheric thermal contrast, contributing to the weakened NAID index. The cross-equator flow is thus weakened, decreasing the NHLMR, which cause a resonant behavior of NHLMR and NAID.

Plain Language Summary Understanding the decadal variability of Northern Hemisphere land monsoon rainfall (NHLMR) is significant for climate predictions, infrastructure construction, food security, water resources planning, and disaster reduction in the monsoon region. However, the secular changes in the decadal relationship between NHLMR and sea surface temperature (SST) over the past millennium are unknown, due to the temporal limitation of observational data. This study explores the decadal relationship between NHLMR and SST in the past millennium through the Community Earth System Model-Last Millennium Ensemble (CESM-LME) simulation data. We use two SST indexes, including the extended El Niño–Southern Oscillation (XEN) SST index and North Atlantic–south Indian Ocean dipole (NAID) SST index. The decadal relationship between NHLMR and XEN has been stable and significant in the past millennium, which is caused by internal variability. However, the decadal relationship between NHLMR and NAID is only significant after 1700. The volcanic forcing experiments show that the successive strong volcanic eruptions in the NH induce the synchronous changes of NHLMR and NAID.

Software: Tianyin Shen
Supervision: Weiyi Sun, Jian Liu
Writing – original draft: Tianyin Shen, Weiyi Sun
Writing – review & editing: Weiyi Sun, Jian Liu, Bin Wang, Deliang Chen

1. Introduction

Northern Hemisphere (NH) land monsoon rainfall (NHLMR) affects more than two-thirds of the world's population, providing water resources for local agriculture and ecosystems (Mohtadi et al., 2016). Understanding the variability of NHLMR is of great significance for climate predictions, infrastructure construction, food security, water resources planning, and disaster reduction in the monsoon region (B. Wang et al., 2021). Progress has been made in detecting the NHLMR change under anthropogenic forcings using observations and simulations from phase 5/6 of the Coupled Model Intercomparison Project (CMIP5/6) (Lee & Wang, 2012; Wang et al., 2020; Zhou et al., 2020). However, the impact of the natural external forcings and internal variability on the decadal NHLMR variability, especially the change of the decadal relationship between NHLMR and sea surface temperature (SST), remains elusive (Meehl et al., 2009).

Much effort has been made in understanding the decadal variations of NHLMR (Sutton & Hodson, 2005; Webster et al., 1998). For example, Goswami et al. (2006) found that the Atlantic Multidecadal Oscillation (AMO) regulates the frequency of the North Atlantic Oscillation or North Annular mode, which affects the decadal change of the Indian summer monsoon (ISM). The linkages between the AMO and Asian, North African, and North American monsoons were also detected (Gaetani & Mohino, 2013; Lu et al., 2006). Some studies pointed out the important role of multidecadal Pacific SST anomalies and the Pacific Decadal Oscillation (PDO) in inducing the megadroughts over the Indian monsoon and Southwest North America and influencing the North China aridity (Meehl & Hu, 2006; Qian & Zhou, 2014). The Pacific Decadal Variability can change the decadal variation of SST in the North and South Pacific, which may also influence the global precipitation (W. Sun, Wang, et al., 2022). Considering the influence of global SST, B. Wang et al. (2013) proposed a combined effect of the mega-El Niño/Southern Oscillation (ENSO) and the AMO on driving the present NH summer monsoon system. Further, B. Wang et al. (2018) found that the decadal change of NHLMR could be predicted about a decade in advance using (a) an extended ENSO (XEN) index representing the east-west SST contrast over the Pacific and (b) a North Atlantic–south Indian Ocean dipole (NAID) index representing the north-south hemispheric thermal contrast. However, it is unclear whether the decadal relationship between the NHLMR and XEN/NAID indices changes over a longer period and how it responds to external forcings.

The past millennium provides a larger sample size and some periods with stronger natural external forcings, which is important to understand the secular change of decadal NHLMR variability. Using the gridded tree-ring data, Hidolgo (2004) found that the interdecadal hydrologic change over the western United States is related to the SST over the North Pacific and the North Atlantic during 1525–1975. Especially, the PDO and AMO had a large explanation power for this interdecadal variability. Some studies found that the centennial variability of the Asian summer monsoon (ASM) is closely related to the NH temperature and meridional thermal gradients (Naidu et al., 2020; Sinha et al., 2015; W. Sun et al., 2017), but this relationship has not been verified on the decadal time scale. Interestingly, during 1720–1800, reconstructions showed that there was a maximum multi-decadal variability of ISM (Sinha et al., 2015), and a significant positive correlation between the ISM and AMO also occurred around the early 18th century (F. Shi et al., 2017). Similarly, a significant relationship between the Asian rainfall and AMO occurred during 1750–1825 while it greatly reduced after 1825 (H. Shi et al., 2019), but the physical mechanism is still unclear.

Climate models provide an opportunity to explore the past changes in the decadal relationship between the NHLMR and SST. Using the simulations conducted with a coupled atmosphere–chemistry–ocean model SOCOL-MPIOM, Malik et al. (2017) found a consistent negative correlation between the ISM and PDO on the decadal-multidecadal time scales over the past 400 years while the ISM-AMO correlation is not stationary. Ying et al. (2018) suggested that PDO and AMO are important factors affecting the decadal precipitation over China during the last millennium using an Earth System model CCSM4. Recently, some modeling studies suggested that the successive volcanic eruptions could significantly influence the multi-decadal variability of AMO and PDO over the past millennium (Dai et al., 2022; Mann et al., 2021; W. Sun, Liu, et al., 2022), which may further affect the ASM (Ning et al., 2017, 2020), drought (K. Chen et al., 2020; K. F. Chen et al., 2022), and megadrought risk over the Amazon and Mexico (Stevenson et al., 2018). However, it remains unknown whether there is a secular change in the decadal relationship between the NHLMR and XEN/NAID indices over the past millennium; if so, what are the roles of internal variability and external forcings in the change?

10.1029/2022JD037065

To address these questions, we use the Community Earth System Model-Last Millennium Ensemble (CESM-LME) simulations with different forcings to explore the secular changes in decadal correlation between the NHLMR and XEN/NAID indices over the past millennium (850–1850). By comparing simulations under all-forcings with those under single-forcing, we aim to explore the roles played by internal variability and external forcings in influencing the changes in decadal relationships.

2. Data and Methodology

2.1. Model Data

The model data used here was derived from the CESM-LME (Otto-Bliesner et al., 2016). The resolution of the model for the atmosphere/land components is ~2° and the resolution for the ocean/sea-ice components is ~1°. The simulations include a pre-industrial control experiment (CTRL), 13 AF experiments (AF), and 18 single-forcing sensitivity experiments including 4 total solar irradiation (TSI) experiments, 5 volcanic eruptions experiments (VOL), 3 greenhouse gas (GHG) experiments, 3 orbital parameter experiments (ORB), and 3 land use/land cover change experiments (LUCC). The main differences between the ensemble members are mainly due to the different perturbations of the small random roundoff (order 10^{-14}°C) changes in the air temperature field (Otto-Bliesner et al., 2016). Thus, the ensemble mean results can be considered as the main contribution of external forcings, while internal variability can be inferred using the results from the CTRL. The volcanic forcing was reconstructed by Gao et al. (2008), which was used to drive the AF and VOL experiments. Previous studies found that in the CESM-LME, the simulated relationship between monsoon precipitation and SST (i.e., AMO and ENSO) is relatively consistent with the reconstructed and observed results (Stevenson et al., 2016, 2018; Zuo et al., 2019).

In addition, to compare with the results from other climate models, the simulation results of Paleoclimate Modeling Intercomparison Project Phase III (PMIP3) over the last millennium were also used (Braconnot et al., 2012), including the CCSM4, FGOALS-s2, MRI-CGCM3, MPI-ESM-P, HadCM3, GISS-E2-R, CSIRO-Mk3L-1-2, and BCC-CSM1-1. It should be mentioned that the volcanic forcing used in the CCSM4, FGOALS-s2, MRI-CGCM3, and BCC-CSM1-1 was derived from the Gao et al. (2008) while the volcanic forcing used in the MPI-ESM-P, HadCM3, GISS-E2-R, and CSIRO-Mk3L-1–2 was derived from the Crowley et al. (2008). Since the spatial resolutions of experiments are different in these models, we first interpolate all the data to a resolution of $2° \times 2°$.

2.2. Observational Data

We also use the observation data to compare with the modeling results. The observational data includes the Global Precipitation Climatology Centre (GPCC) with a resolution of $1° \times 1°$ during 1901–2014 and the National Oceanic and Atmospheric Administration (NOAA) Extended Reconstructed SST version 5 (ERSST.v5) with a resolution of $2° \times 2°$ during 1901–2014.

2.3. Definitions of NHLMR, XEN, and NAID Indices

According to the definition by Wang and Ding (2008), the NH monsoon region is defined as the local rainfall in summer on the land that exceeds 55% of the annual rainfall, and the annual rainfall difference (the difference between summer rainfall rate and winter rainfall rate) exceeds 2 mm day^{-1}, where summer is defined as May to September (MJJAS), and winter is defined as November to March of the next year. The NH land monsoon regions include the North African monsoon, South Asian monsoon, East Asian monsoon, and North American monsoon. In this paper, the NHLMR index is defined by the area-weighted average of MJJAS mean precipitation over the NH land monsoon region, which can be used to measure the intensity of the NH land monsoon (B. Wang et al., 2018).

Besides, to verify the capture ability of CEMS-LME to the NH monsoon region, we use GPCC and CESM-LME by the above definition during 1901–2000 to compare the NH monsoon region between observation and simulation data (Figure S1 in Supporting Information S1). It shows the NH monsoon region in GPCC and CESM-LME is almost the same.

10.1029/2022JD037065

To examine the correlation between the NHLMR and the associated SST change on the decadal time scale, we define two SST indices according to B. Wang et al. (2018). One is the extended ENSO (XEN) index representing the east-west SST contrast over the Pacific, which is significantly correlated with the NHLMR ($r = 0.53$, $p < 0.05$) on the decadal time scale during 1901–2014. The XEN index can be defined by the SST anomaly (SSTA) over the K-shaped Western Pacific region minus the SSTA over the triangular region in the eastern Pacific (B. Wang et al., 2018), which is shown as follow:

$$\text{XEN index} = \text{SSTA(WP K\_shaped region)} - \text{SSTA(EP triangle region)} \quad (1)$$

The other one is the NAID index. The NAID index indicates the Northern Hemisphere-Southern Hemisphere (NH-SH) hemispheric thermal contrast over the Atlantic–Indian Ocean sector, which has also a significant correlation with the NHLMR during 1901–2014 ($r = 0.68$, $p < 0.05$). The NAID index is defined by the difference between the SSTA over the North Atlantic region (0°–60°N, 80°W–0°) and the SSTA over the southern Indian Ocean (0°–40°S, 50°E−110°E):

$$\text{NAID index} = \text{SSTA (NA)} - \text{SSTA (SIO)} \quad (2)$$

3. Secular Changes in the Decadal Relationship Between the NHLMR and XEN/NAID Indices Over the Past Millennium

To identify the relationship between the NHLMR and XEN/NAID indices over the past millennium, we first analyze the rolling correlations with 100-year windows between the 5-year running mean NHLMR and XEN/NAID indices, deriving from 13 AF experiments in the CESM-LME (Figure 1). For example, the value in the year 1000 represents the correlation coefficient during 951–1050. The result shows that almost all AF experiments show a robust and significant correlation between the NHLMR and XEN indices during the last millennium (Figures 1a–1m), where the effective degree of freedom is about 22 according to the calculation of Bretherton et al. (1999). As a result, the AF ensemble means result further shows significant correlations ranging from 0.5 to 0.6 (Figure 1n). This means that the CESM-LME produces a significant decadal correlation between the NHLMR and XEN indices in almost any period, and the external forcings do not have a strong influence on the relationship.

To check if and how the NHLMR-XEN relationship is influenced by internal variability, we analyze results from the 1,000-year CTRL experiment (Figure 2). We find that the correlation coefficient between the NHLMR and XEN indices is also significant for most of the 1,000 years, with coefficients ranging from approximately 0.4 to 0.6. Generally, a decadal relationship between the NHLMR and XEN indices is similarly stimulated by the CTRL which is only influenced by internal variability.

Next, we investigate the secular changes in the decadal correlation coefficient between the NHLMR and NAID indices over the past millennium. Most of the AF members suggest that insignificant correlations happen most of the time, excepting the significant increase after 1700 (Figures 1a–1m), where the effective degree of freedom is about 17. Particularly, 12 of 13 AF members show significant NHLMR-NAID correlations ranging from 0.4 to 0.6 around 1740. The ensemble means result also suggests a prominent NHLMR-NAID correlation emerged after 1700, with a peak around 1740 (Figure 1n), while a reduction occurs at the end of the 18th century. Additionally, 7 of 13 AF members show significant NHLMR-NAID correlations ranging from 0.4 to 0.6 around 1210, but the ensemble means result suggests an insignificant NHLMR-NAID correlation around 1210.

This NHLMR-NAID correlation change has also been inferred from reconstructions. H. Shi et al. (2019) reconstructed the Asian rainfall data during 1470–2013 and found that the Asian rainfall has a strong decadal signal after 1700, coinciding with an ISM record (Sinha et al., 2015). Compared with AMO reconstructions (Mann et al., 2009; Steiger et al., 2018; J. Wang et al., 2017), H. Shi et al. (2019) further found a significant relationship between the Asian rainfall and AMO during 1750–1825, and this relationship greatly reduced after 1825. Meanwhile, F. Shi et al. (2017) also found that a significant positive correlation between the ISM and AMO occurred around the early 18th century and after the late 19th century. In addition, we also calculated the relationship between ASM and AMO since 1700 using CESM-LME data. The relationship is highly correlated and significant from 1720 to 1800, which is very similar to previous reconstructions (e.g., Fig 9 in H. Shi et al., 2019, figure not shown). These reconstructions verify the reliability of the CESM-LME results. However, due to the lack of

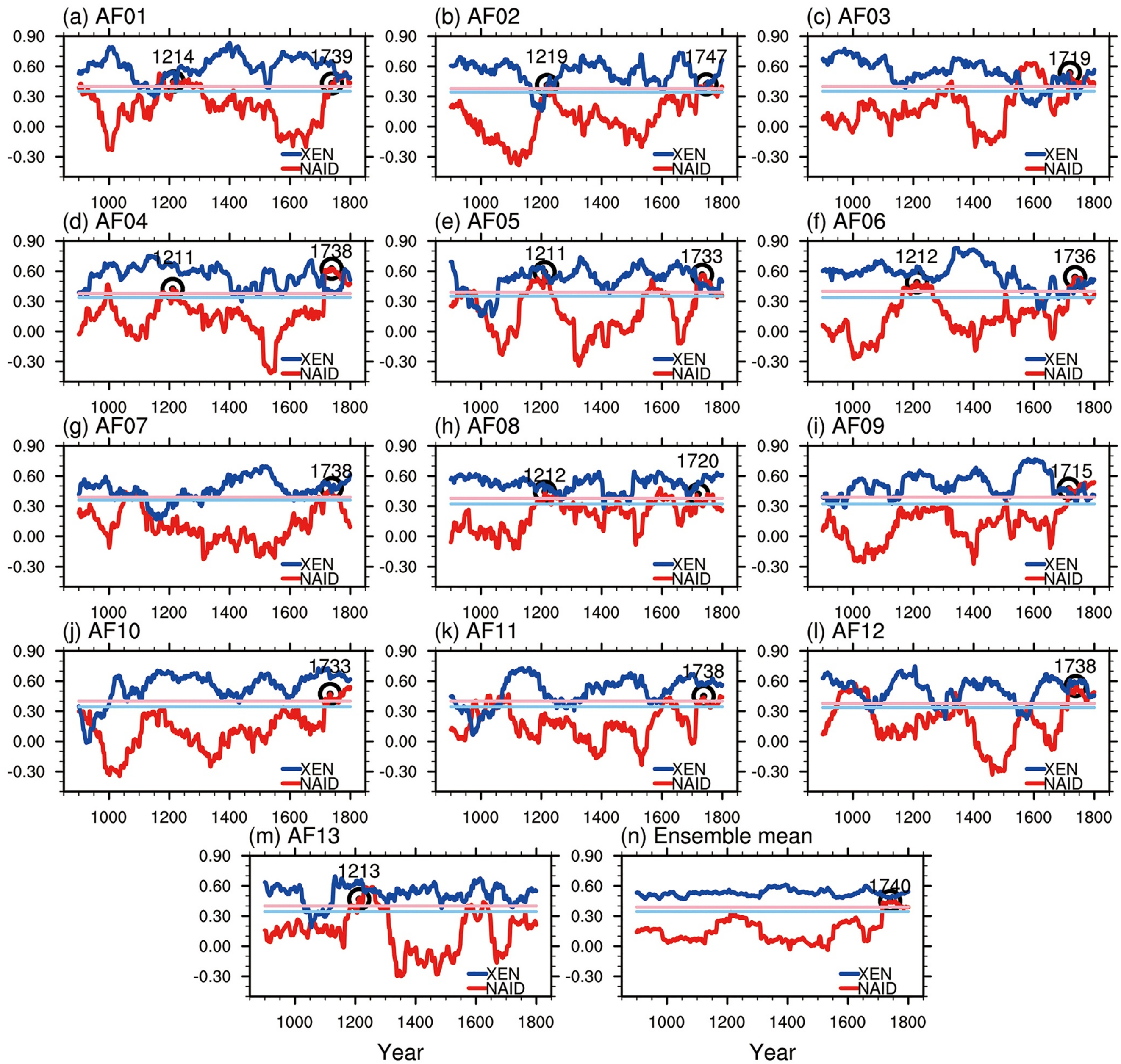

Figure 1. The rolling correlation coefficient between Northern Hemisphere land monsoon rainfall (NHLMR) and North Atlantic–south Indian Ocean dipole (NAID)/extended El Niño–Southern Oscillation (XEN) indices with a 100-year window during 850–1850 in the all-forcing simulations. The 5-year running mean is used before analysis. (a–m) Result from each experiment. (n) The ensemble-mean result. The effective degree of freedom between NHLMR and NAID is about 17, while the effective degree of freedom between NHLMR and XEN is about 22 (Bretherton et al., 1999). The thin red and blue lines are the correlation coefficients at the 90% significant level. 12 of 13 experiments passed the 90% significant level around 1740, and 7 of 13 passed the 90% significant level around 1210.

high-resolution data over the other monsoon regions and the southern Indian Ocean, the simulated NHLMR-NAID correlation change still has some uncertainty and needs to be studied in the future.

To check if the NHLMR-NAID relationship can be influenced by internal variability, results from the CTRL experiment were examined (Figure 2). We do not find any significant correlation coefficient between the NHLMR and NAID indices on the decadal time scale. This modeling result suggests that the internal variability may not significantly affect the NHLMR-NAID relationship.

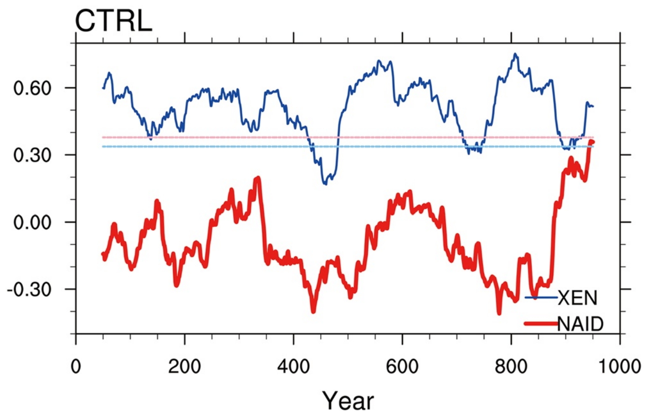

Figure 2. The rolling correlation coefficient between Northern Hemisphere land monsoon rainfall and North Atlantic–south Indian Ocean dipole/extended El Niño–Southern Oscillation indices with a 100-year window during 850–1850 in the control experiment. The 5-year running mean is used before analysis. The thin red and blue lines are the correlation coefficients at the 90% significant level.

Overall, we speculate that the reason why the simulated NHLMR-NAID relationship becomes significant after 1700 in the AF experiments can be induced by external forcings. Consequently, the next question is: which external forcing contributes to that?

4. Can Northern Hemisphere Volcanic Eruptions Affect the NHLMR-NAID Relationship?

First, we examine the two relationships in the volcanic-forcing (VOL) sensitive experiments (Figure 3). The result shows that a significant positive correlation between the NHLMR and NAID index occurs around 1220 and after 1700, inferred from the 4 of 5 VOL experiments (Figures 3a–3e), which is also suggested by the VOL ensemble mean result (Figure 3f). The NHLMR-NAID relationship is higher during 1720, relative to that during 1220. This result is consistent with the result in the AF experiments, which means that the volcanic forcing plays an important role in strengthening the NHLMR-NAID relationship after 1700.

To investigate the impact of other external forcings, the results of the GHG, LUCC, ORB, and TSI sensitivity experiments have been used (Figure 4). Each ensemble member, as well as their ensemble means, shows the insignificant correlation between the NHLMR and NAID indices over the past

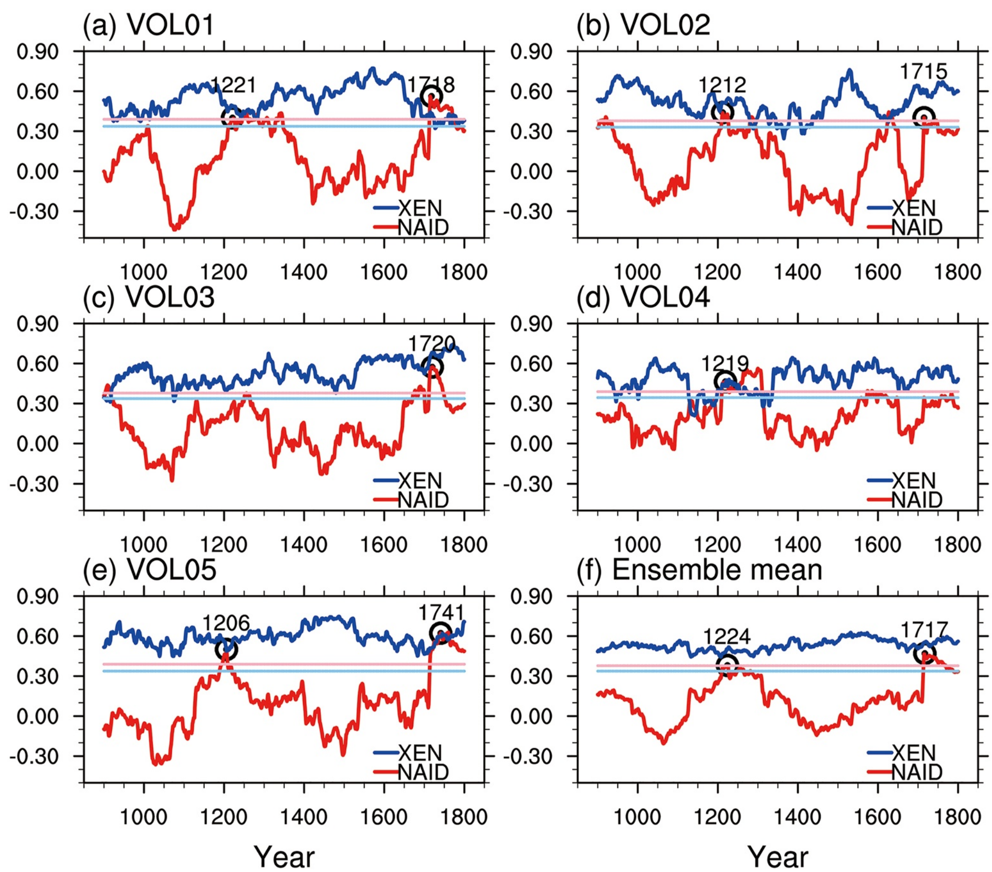

Figure 3. Same as Figure 1, but for the results in the VOL simulations (a–e) Result from each experiment. (f) The ensemble-mean result. The thin red and blue lines are the correlation coefficients at the 90% significant level. 4 of the 5 experiments pass the 90% significant level around 1740 and 1210.

10.1029/2022JD037065

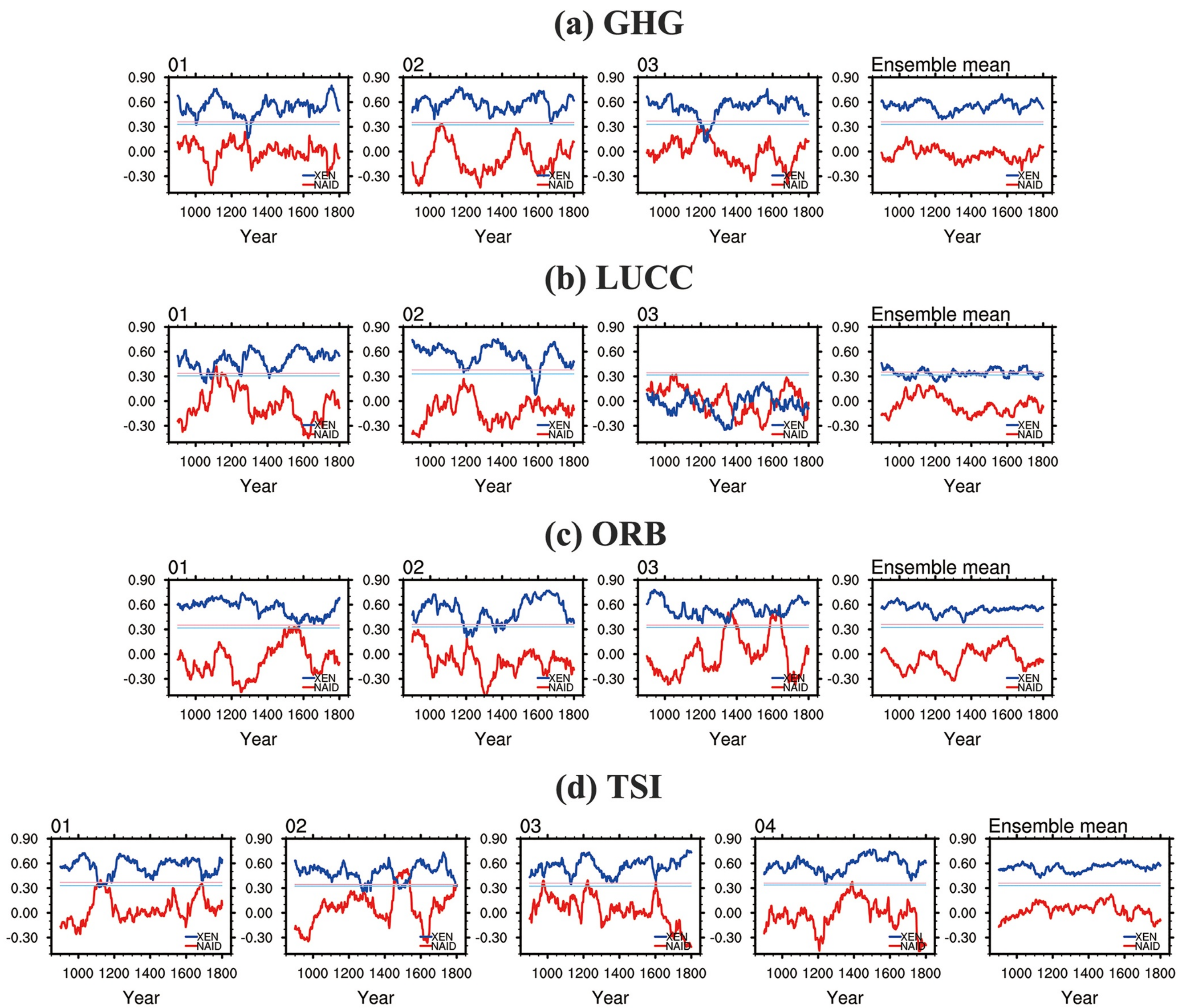

Figure 4. Same as Figure 1, but for the results in the greenhouse gas (a), land use/land cover change experiments (b), orbital parameter experiment (c), and total solar irradiation (d) simulations, respectively. The last panel in each row represents the ensemble mean result.

1000 years under the effect of GHG, LUCC, ORB, and TSI. This means that the GHG, LUCC, ORB, and TSI forcings do not have a significant influence on the NHLMR-NAID relationship over the past millennium.

Next, we reveal the specific temporal variations of the NHLMR and NAID indices derived from the AF and VOL experiments and space-time evolutions of volcanic aerosol during 1162–1261 (period of weak positive correlation) and 1690–1789 (period of significant positive correlation) (Figure 5). In these two periods, volcanic eruptions are strong and frequent. During 1162–1261, the ensemble mean NHLMR shows obvious reductions during 1176–1179, 1210–1215, and 1257–1263 in both of the AF and VOL experiments (Figures 5a and 5c), which can be related to the strong tropical and NH volcanic eruptions (Figures 5e and 5g). Correspondingly, there are also reductions in the NAID index but the intensities are relatively weak. During 1690–1789, the simulated NHLMR and NAID indices show significant reductions during 1716–1724 and 1761–1770 (Figures 5b and 5d), influenced by strong NH volcanic eruptions (Figures 5f and 5h). Comparing the latitude locations of volcanic eruptions during these two periods, we find that the strong and successive NH volcanic eruptions induce more synchronous changes in the NHLMR and NAID indices. We also calculate the correlation of NHLMR-NAID after removing those two mega volcanic eruptions of 1258 and 1763 events, and the correlations during 1162–1261 and

Journal of Geophysical Research: Atmospheres

10.1029/2022JD037065

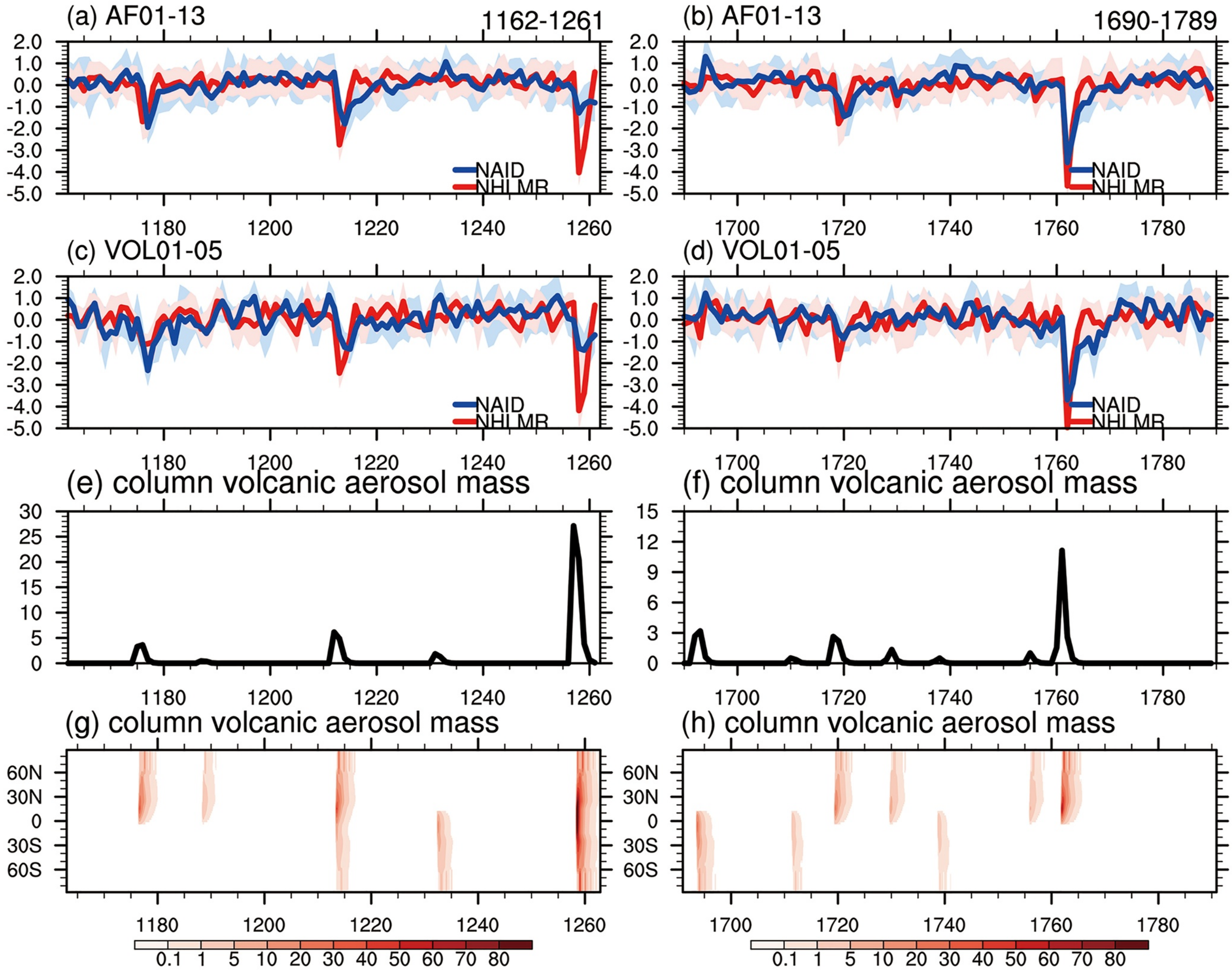

Figure 5. Temporal variations of Northern Hemisphere land monsoon rainfall (NHLMR) and North Atlantic–south Indian Ocean dipole (NAID) indices during two active volcanic periods. (a and b) Time series of the ensemble mean NHLMR and NAID indices during 1162–1261 and 1690–1789 in the all-forcing experiments, respectively. Shadings represent one standard deviation. (c and d) are the same as (a and b), but for the results in the VOL experiments. (e and f) Time series of the column volcanic aerosol mass (10^5 kg m^{-2}) during 1162–1261 and 1690–1789, respectively. (g and h) Latitude-time evolutions of the column volcanic aerosol mass (10^5 kg m^{-2}) during 1162–1261 and 1690–1789, respectively.

1690–1789 are still significant. However, the strong and successive NH volcanic eruptions do not significantly affect the variation of the XEN index (Figure S2 in Supporting Information S1).

Since volcanic eruptions induce the reductions in both NHLMR and NAID indices, we further check their decadal periodicity changes under volcanic forcing over the past millennium, especially during 1690–1789. Wavelet analysis of the temporal variation of the spectra reveals a sudden change in the NHLMR's decadal periodicity and intensity around 1162–1261 and 1690–1789 across most of the AF and VOL simulations (Figures 6 and 7). During these two periods, the NHLMR's variance with the prominent 20–40-year periodicities sharply increases. In contrast, during other times, the NHLMR is weak and lacks a coherent decadal periodicity. Similarly, the AF and VOL-forced NAID index also indicate significant 20–40-year periodicities during these two periods, especially for 1690–1789, in the most member runs and their ensemble mean result (Figures S3 and S4 in Supporting Information S1). This means that the successive strong volcanic eruptions induce the synchronous decadal-scale cycles of the NHLMR and NAID indices. Meanwhile, the XEN index does not have significant 20–40-year cycles over the past millennium under the AF or volcanic forcing (Figures S5 and S6 in Supporting Information S1).

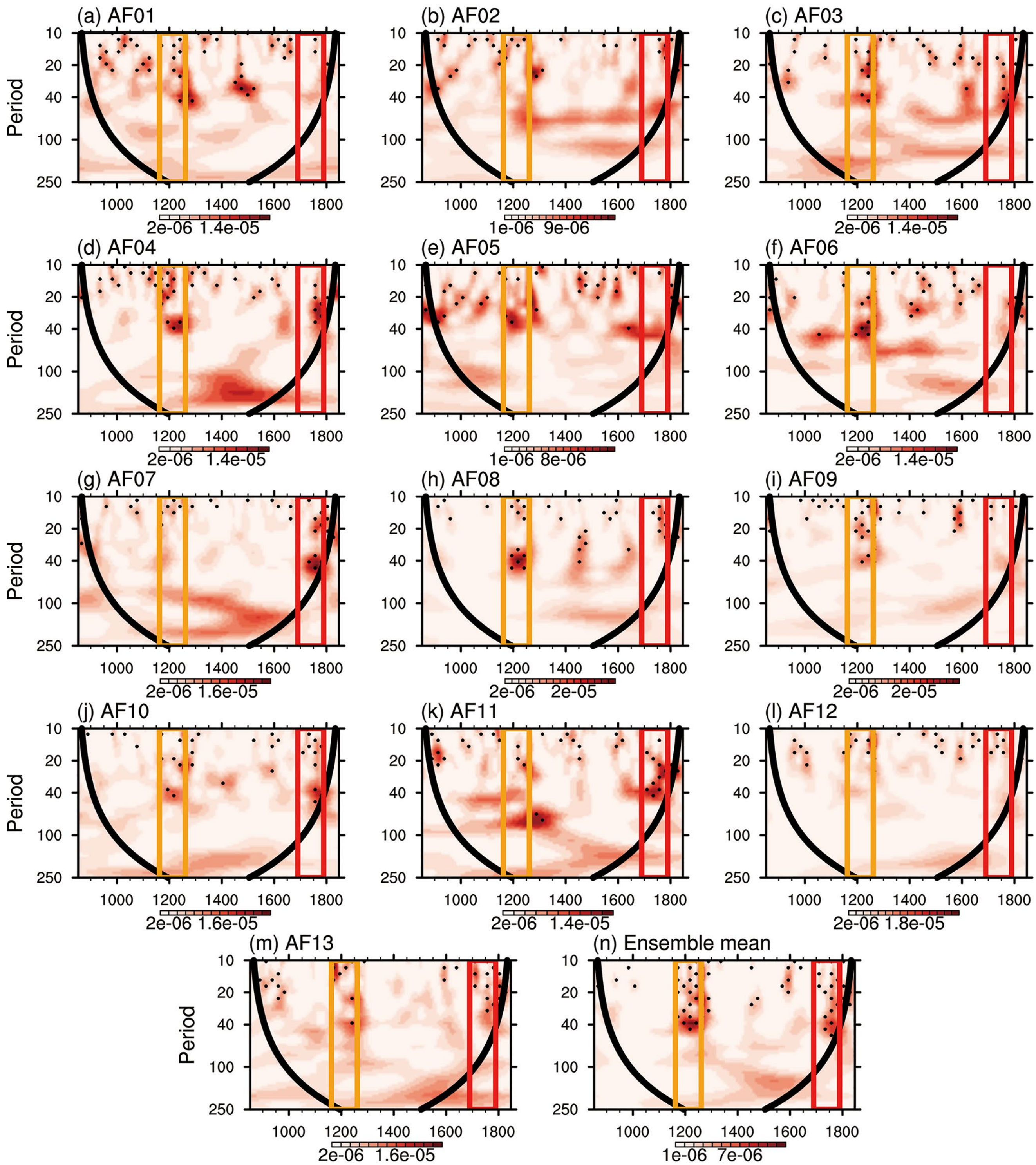

Figure 6. Wavelet analysis of the Northern Hemisphere land monsoon rainfall during 850–1850 in the 13 all-forcing experiments (a–m) and their ensemble mean result (n). The 5-year running mean is used before analysis. The red box marks the period of 1690–1789, while the orange box marks the period of 1162–1261. The black dots denote significance at the 90% confidence level.

Due to the small number of CESM-LME VOL experiments, there may be large uncertainty in directly calculating the relative contribution of volcanic eruptions and internal variability to the relationship. We further check the contributions of NAID/XEN on the NHLMR under internal variability and volcanic eruptions, respectively, by

10.1029/2022JD037065

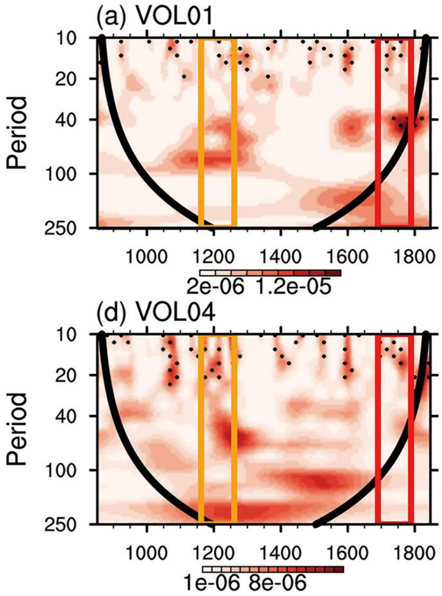

Figure 7. (a–e) Wavelet analysis of the Northern Hemisphere land monsoon rainfall during 850–1850 in the 5 VOL experiments and (f) their corresponding ensemble mean result. The 5-year running mean is used before analysis. The red box marks the period of 1690–1789, while the orange box marks the period of 1162–1261. The black dots denote significance at the 90% confidence level.

calculating the regression coefficients of NHLMR on the NAID/XEN indices during 1690–1789. Figure 8 shows that the one degree Celsius increase in the XEN may cause an increase in the NHLMR by 0.62 mm day^{-1} in the CTRL experiment, which is similar to the AF and VOL experiments. This means that internal variability plays a dominant role in the NHLMR-XEN relationship and volcanic forcings have no obvious effect. 1°C increase in

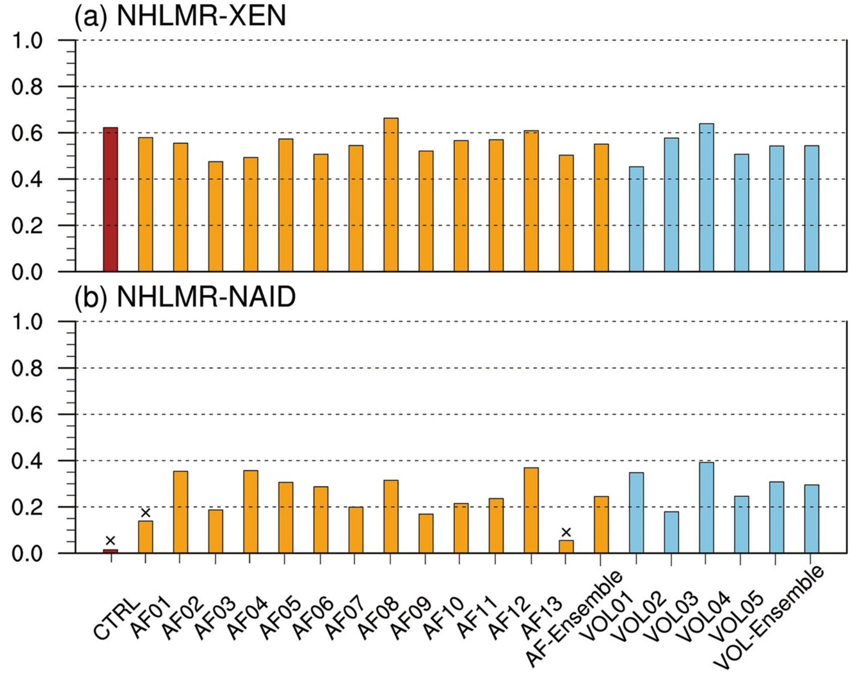

Figure 8. The bar graph of the coefficients (mm day^{-1} °C^{-1}) of Northern Hemisphere land monsoon rainfall regressed onto the North Atlantic–south Indian Ocean dipole/extended El Niño–Southern Oscillation indices during 1690–1789, respectively. The red bar represents the control (CTRL) experiment. The ordinate unit is mm day^{-1}. The orange bars represent all-forcing (AF) experiments and the blue bars represent VOL experiments. They all pass the 90% significant level, except CTRL, all-forcing 01, and AF13 in (b), marked by "×."

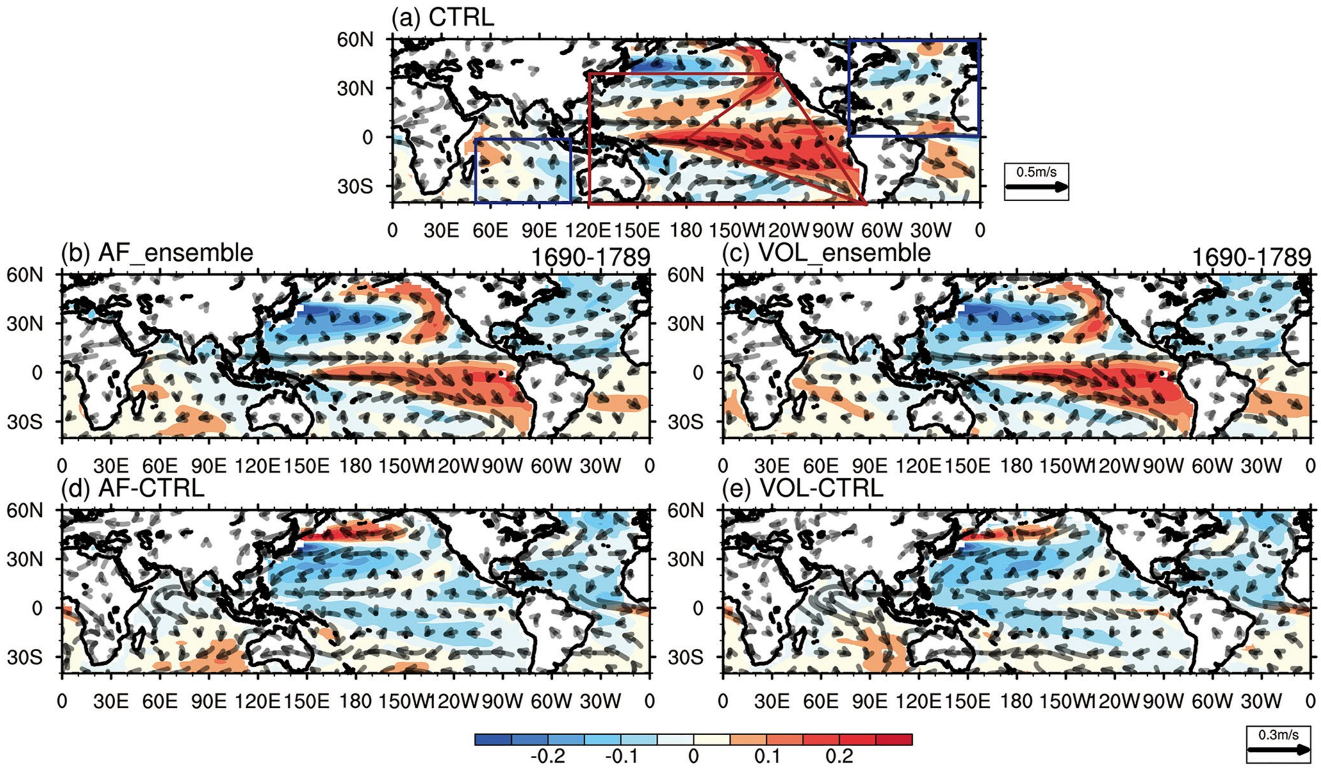

Figure 9. The regression result of the 850 hPa winds (vectors; m s^{-1}) and sea surface temperature (shading; °C) on the Northern Hemisphere land monsoon rainfall. (a) Result in the control (CTRL) experiment. (b) Result during 1690–1789 in the all-forcing (AF) experiment. (c) Result during 1690–1789 in the VOL experiment. The vector unit of winds in (a–c) is 0.5 m s^{-1}. (d) Difference between the results in the AF and CTRL runs ((b) minus (a)); (e) Difference between the results in the VOL and CTRL runs ((c) minus (a)). The results are multiplied by −1 to reflect the variability under volcanic forcing. The vector unit of winds in (d and e) is 0.3 m s^{-1}. The blue boxes mark the region of North Atlantic–south Indian Ocean dipole, while the pink boxes mark the region of extended El Niño–Southern Oscillation.

the NAID may not induce any significant change (0.02 mm day^{-1}) in NHLMR in the CTRL experiment, while it induces increases in the NHLMR by 0.25 and 0.29 mm day^{-1} in the AF and VOL experiments, respectively. This means that, under strong and successive NH volcanic forcing, the NAID may significantly contribute to the NHLMR.

To examine how volcanic eruption can influence the synchronous changes of NHLMR and NAID during 1690–1789, we investigate the fields of SST and 850 hPa winds regressed onto the NHLMR in the CTRL, AF, and VOL experiment. To highlight the influence of volcanic forcing, the regression results in the figure need to be multiplied by −1. In the CTRL experiment, the XEN SSTA pattern occurs but the NAID SSTA pattern almost disappears (Figure 9a). During 1690–1789, both the AF and VOL experiments indicate the significant XEN and NAID SSTA patterns, suggesting the important role of active volcanic forcing in modulating the NAID (Figures 9b and 9c). We further compare the results of AF minus CTRL and VOL minus CTRL and find that the cooling (warming) over the North Atlantic and western North Pacific (southern Indian Ocean) is weakened (Figures 9d and 9e). The average anomalous meridional winds over the equatorial Indian Ocean (5°S–5°N, 40–110°E) and the Atlantic Ocean (5°S–5°N, 80°W–0°) are −0.05 and −0.02 m s^{-1}, respectively. This indicates that the cross-equator winds are weakened over the equatorial Indian Ocean and the Atlantic Ocean, which enhances the ASM and the West African monsoon.

According to reconstructed volcanic forcing (Gao et al., 2008), volcanic eruptions in the NH before 1700 were weak and less successive, which fail to induce a significant decadal correlation between NHLMR and NAID. While during 1690–1789, under the successive NH volcanic eruptions, cooling occurs over the North Atlantic and western North Pacific, causing the weakened north-south hemispheric thermal contrast (thus weakened NAID) during boreal summer, thereby decreasing the cross-equator flow and the NH monsoon rainfall (Liu et al., 2016). Meanwhile, the NH volcanic eruptions may also induce the NH cooling and weaken the land-sea thermal contrast, which reduces the specific humidity and atmospheric circulation over the NH monsoon region, respectively, further weakening the NH monsoon precipitation (Zuo et al., 2019). Therefore, the successive NH volcanic eruptions reduce the NHLMR and NAID SSTA at the same time, strengthening the "resonant'' behavior of NHLMR and NAID indices.

To verify the changes in NH-SH thermal contrast under volcanic forcing between 1690 and 1789, we further investigate the fields of surface temperature regressed onto the NHLMR in the CTRL, AF, and VOL experiments. In the CTRL experiment, the difference between the NH and SH is not significant (Figure S7a in Supporting Information S1). Under the influence of volcanic forcing, we find that during 1690–1789, both the AF and VOL experiments indicate strong cooling in the NH (Figures S7b and S7c in Supporting Information S1). We further compare the results of AF minus CTRL and VOL minus CTRL and find that the cooling over the NH and the warming over the SH is enhanced (Figures S7d and S7e in Supporting Information S1). When we calculate the difference between NH and SH, the result of NH minus SH is −0.07°C under AF minus CTRL (Figure S7d in Supporting Information S1) and −0.06°C under VOL minus CTRL (Figure S7e in Supporting Information S1), respectively. This means that the NH volcanic eruptions cause the NH cooling, inducing a "NH-cooler-than-SH" pattern.

5. Discussion

As the study is model-based, one may concern if the CESM-LME can underestimate the relationship between the NHLMR and NAID index in the CTRL experiment (under internal variability). Currently, there are some uncertainties in the simulated decadal variability and the teleconnection between oceanic mode and land precipitation (Li et al., 2017; Otto-Bliesner et al., 2016; Stevenson et al., 2018; C. Sun et al., 2018). The important implications of this work lie in the significant "resonant'' behavior of NHLMR and NAID under volcanic forcing, especially for the NH eruptions. Compared with the CESM-LME and proxy data, Stevenson et al. (2018) also indicated that the volcanic forcing plays an important role in enhancing AMO amplitude, which may further alter the megadrought risk. Meanwhile, comparing the reconstructions of Asian/ISM and AMO, some studies also found a strengthened decadal relationship between the Asian rainfall and AMO around the early 18th century (F. Shi et al., 2017, 2019). However, Rustic et al. (2015) found a "Mid-Millennium Shift" from a state with enhanced zonal gradient and weakened ENSO to one with reduced gradient and intensified ENSO during ~1500–1650 CE, which might be caused by a cooling-induced southward movement of the Intertropical Convergence Zone. Their work found that the transition time was earlier than our result, suggesting the uncertainties in models and reconstructions.

To verify the robustness of our findings, we compare the NHLMR-XEN and NHLMR-NAID relationships from CESM-LME and observational data during the modern day (1901–2000). The NHLMR-NAID and NHLMR-XEN relationships from observational data are both significant. In CESM-LME, there are 12/13 experiments showing a significant NHLMR-XEN relationship, while 7/13 experiments show a significant NHLMR-NAID relationship. We select the seven best simulations, including AF03, AF04, AF05, AF06, AF08, AF11, and AF13, which show significant relationships between NHLMR and NAID during 1901–2000 and explore their simulating NHLMR-NAID/XEN relationships over the past millennium. The results in these seven best experiments are also very similar to the ensemble mean result of CESM-LME (Figure 1n). Overall, the CESM-LME can capture the decadal relationship between the NHLMR and SST mode, compared with observation.

Then, we check some other models' results from the PMIP3 past 1,000 simulations (Braconnot et al., 2012) (Figure 10). Although Each model has different internal variability and the relationship between monsoon precipitation and SST, at least four models (CCSM4, BCC-CSM1-1, CSIRO-Mk3L-1-2, and HadCM3) in PMIP3 show that there is a relatively stable and significant relationship between NHLMR and XEN over the past millennium. In all models, whether the NHLMR-XEN relationship is significant or not, this relationship may not be affected by natural external forcing (i.e., volcanic eruptions). This result is consistent with our results using the CESM-LME.

Next, we find that the significant decadal correlation coefficient between NHLMR and NAID occurred especially around 1740 in the FGOALS-s2, CCSM4, and MRI-CGCM3 but it did not appear in the BCC-CSM1-1 (Figures 10a–10d). The volcanic forcing of these four experiments is reconstructed by Gao et al. (2008), which is the same as the CESM-LME. Further, we also compare simulations from the different settings of volcanic forcing (Crowley et al., 2008), and the result shows that the significant NHLMR-NAID correlation also occurs

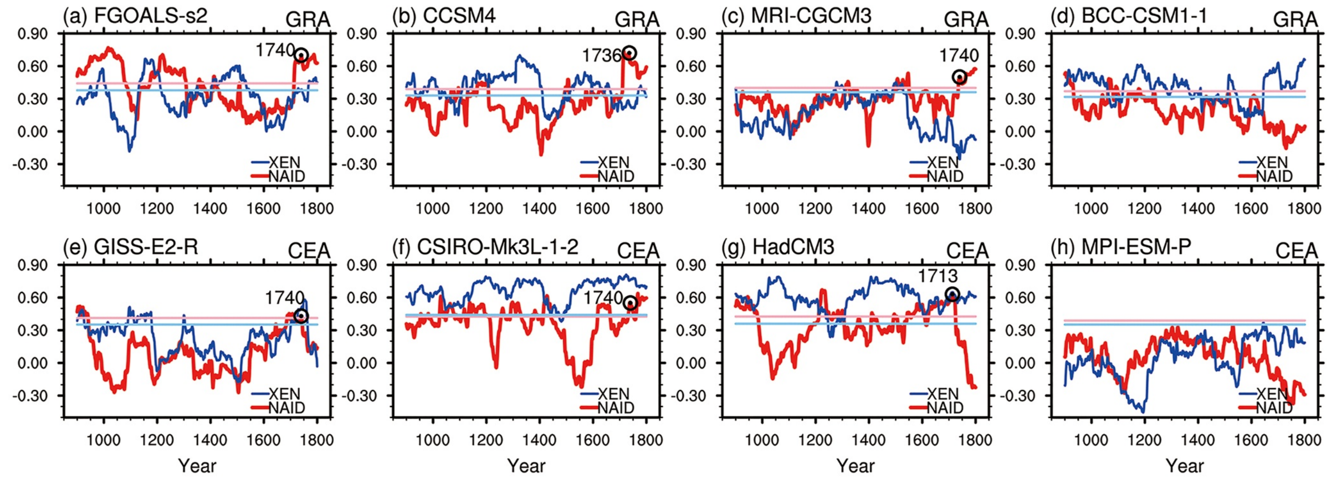

Figure 10. The rolling correlation coefficient between Northern Hemisphere land monsoon rainfall and North Atlantic–south Indian Ocean dipole/extended El Niño–Southern Oscillation indices with a 100-year window during 850–1850 was derived from the Paleoclimate Modeling Intercomparison Project Phase 3 simulations. The 5-year running mean is used before analysis (a–d) The result from the FGOALS-s2, CCSM4, MRI-CGCM3, and BCC-CSM1-1, respectively. These simulations are driven by the volcanic forcing of Gao et al. (2008) (GRA). (e–f) The result from the GISS-E2-R, CSRIO-Mk3L-1-2, HadCM3, and MPI-ESM-P, respectively. These simulations are driven by the volcanic forcing of Crowley et al. (2008) (CEA). The thin red and blue lines are the correlation coefficients at the 90% significant level. 6 of the 8 models passed the significant level around 1740.

at 1740 or 1713 in the GISS-E2-R, CSIRO-Mk3L-1-2, and HadCM3, while it does not occur in the MPI-ESM-P (Figures 10e–10h). Due to the model uncertainty, different models have had distinctive NHLMR-NAID relationships over the past millennium. We speculate that the differences may be caused by SST changes, especially the response of SST to external forcing in the Atlantic and Indian Oceans. The SST change may lead to the instability of the NHLMR-NAID relationship. Although there are differences between models, most of them (6/8) suggest the significant and relatively higher NHLMR-NAID correlation coefficient around 1740, which provides robust and independent support for the contribution of successive NH volcanic eruptions identified in this work.

6. Conclusions

This paper investigates the secular changes in the decadal relationship between the NHLMR and XEN/NAID indices and their influencing factors over the past millennium using the CESM-LME AF and single-forcing sensitivity simulations. The following are the major findings. First, over the past millennium, the simulated relationship between the NHLMR and XEN has always been robust and significant, as found in the AF and CTRL experiments, implying that the NHLMR-XEN relationship is dominated by internal variability. Second, the AF experiments show that the decadal relationship between NHLMR and NAID is practically non-existent until the abrupt and significant increase after 1700. By comparing the CTRL with VOL experiments, we find that successive strong NH volcanic eruptions play an important role in that change, inducing the 20–40-year periodicities of NHLMR and NAID and promoting the synchronization of their variabilities. Third, the physical process behind the emerged relationship between NHLMR and NAID is that the NH volcanic eruptions weaken the north-south hemispheric thermal contrast, inducing an "NH-cooler-than-SH" pattern (a weakened NAID index). Then, the cross-equator flow is reduced, decreasing the NHLMR, which leads to the synchronous negative phase of NHLMR and NAID on the decadal scale.

Conflict of Interest

The authors declare no conflicts of interest relevant to this study.

10.1029/2022JD037065

Data Availability Statement

The observations from the Global Precipitation Climatology Centre and NOAA Extended Reconstructed SST V5 are freely available through NOAA (2011) and NOAA (2017). The simulations from the Community Earth System Model (CESM) Last Millennium Ensemble (LME) Project are freely available through Otto-Bliesner et al. (2016) and NCAR (2016). The simulations used in Paleoclimate Modeling Intercomparison Project Phase III/phase 5 of Coupled Model Intercomparison Project LM experiment (PMIP, 2020) is used to be compared with the results of CESM-LME.

Acknowledgments

We thank the Global Precipitation Climatology Centre, Extended Reconstructed sea surface temperature, Community Earth System Model (CESM) Last Millennium Ensemble (LME), and Paleoclimate Modeling Intercomparison Project Phase III for providing the observation and modeling data. Our study was supported by the National Natural Science Foundation of China (Grant 42130604, 42105044, 41971108, 42111530182, and 91437218) and Swedish STINT (Grant CH2019-8377).

References

Braconnot, P., Harrison, S. P., Kageyama, M., Bartlein, P. J., Masson-Delmotte, V., Abe-Ouchi, A., et al. (2012). Evaluation of climate models using palaeoclimatic data. *Nature Climate Change*, *2*(6), 417–424. https://doi.org/10.1038/nclimate1456

Bretherton, C. S., Widmann, M., Dymnikov, V. P., Wallace, J. M., & Bladé, I. (1999). The effective number of spatial degrees of freedom of a time-varying field. *Journal of Climate*, *12*(7), 1990–2009. https://doi.org/10.1175/1520-0442(1999)012<1990:tenosd>2.0.co;2

Chen, K., Ning, L., Liu, Z., Liu, J., Yan, M., Sun, W., et al. (2022). Nonlinear responses of droughts over China to volcanic eruptions at different drought phases. *Geophysical Research Letters*, *49*(4). https://doi.org/10.1029/2021gl096454

Chen, K. F., Ning, L., Liu, Z., Liu, J., Yan, M., Sun, W., et al. (2020). One drought and one volcanic eruption influenced the history of China: The Ming Dynasty mega-drought. *Geophysical Research Letters*, *47*(16). https://doi.org/10.1029/2020gl088124

Crowley, T. J., Zielinski, G., Vinther, B., Udisti, R., Kreutz, K., Cole-Dai, J., & Castellano, E. (2008). Volcanism and the Little Ice Age. *PAGES Newsletter*, *16*(2), 22–23. https://doi.org/10.1029/2002GL0166335

Dai, Z., Wang, B., Zhu, L., Liu, J., Sun, W., Li, L., et al. (2022). Atlantic multidecadal variability response to external forcing during the past two millenniums. *Journal of Climate*, *35*(24), 1–27. https://doi.org/10.1175/jcli-d-21-0986.1

Gaetani, M.,& Mohino, E. (2013). Decadal prediction of the Sahelian precipitation in CMIP5 simulations. *Journal of Climate*, *26*(19), 7708–7719. https://doi.org/10.1175/jcli-d-12-00635.1

Gao, C., Robock, A., & Ammann, C. (2008). Volcanic forcing of climate over the past 1500 years: An improved ice core-based index for climate models. *Journal of Geophysical Research*, *113*(D23), D23111. https://doi.org/10.1029/2008jd010239

Goswami, B. N., Madhusoodanan, M. S., Neema, C. P., & Sengupta, D. (2006). A physical mechanism for North Atlantic SST influence on the Indian summer monsoon. *Geophysical Research Letters*, *33*(2), L02706. https://doi.org/10.1029/2005gl024803

Hidalgo, H. G. (2004). Climate precursors of multidecadal drought variability in the Western United States. *Water Resources Research*, *40*(12). https://doi.org/10.1029/2004wr003350

Lee, J.-Y., & Wang, B. (2012). Future change of global monsoon in the CMIP5. *Climate Dynamics*, *42*(1–2), 101–119. https://doi.org/10.1007/s00382-012-1564-0

Li, J., Zhu, Z., & Dong, W. (2017). Assessing the uncertainty of CESM-LE in simulating the trends of mean and extreme temperature and precipitation over China. *International Journal of Climatology*, *37*(4), 2101–2110. https://doi.org/10.1002/joc.4837

Liu, F., Chai, J., Wang, B., Liu, J., Zhang, X., & Wang, Z. (2016). Global monsoon precipitation responses to large volcanic eruptions. *Scientific Reports*, *6*(1), 24331. https://doi.org/10.1038/srep24331

Lu, R., Dong, B., & Ding, H. (2006). Impact of the Atlantic Multidecadal Oscillation on the Asian summer monsoon. *Geophysical Research Letters*, *33*(24), L24701. https://doi.org/10.1029/2006gl027655

Malik, A., Brönnimann, S., Stickler, A., Raible, C. C., Muthers, S., Anet, J., et al. (2017). Decadal to multi-decadal scale variability of Indian summer monsoon rainfall in the coupled ocean-atmosphere-chemistry climate model SOCOL-MPIOM. *Climate Dynamics*, *49*(9–10), 3551–3572. https://doi.org/10.1007/s00382-017-3529-9

Mann, M. E., Steinman, B. A., Brouillette, D. J., & Miller, S. K. (2021). Multidecadal climate oscillations during the past millennium driven by volcanic forcing. *Science*, *371*(6533), 1014–1019. https://doi.org/10.1126/science.abc5810

Mann, M. E., Steinman, B. A., Brouillette, D. J., Miller, S. K., Hughes, M. K., Shindell, D., et al. (2009). Global signatures and dynamical origins of the little ice age and medieval climate anomaly. *Science*, *326*(5957), 1256–1260. https://doi.org/10.1126/science.1177303

Meehl, G. A., & Hu, A. (2006). Megadroughts in the Indian monsoon region and southwest North America and a mechanism for associated multidecadal Pacific sea surface temperature anomalies. *Journal of Climate*, *19*(9), 1605–1623. https://doi.org/10.1175/JCLI3675.1

Meehl, G. A., Hu, A., & Santer, B. D. (2009). The Mid-1970s climate shift in the pacific and the relative roles of forced versus inherent decadal variability. *Journal of Climate*, *22*(3), 780–792. https://doi.org/10.1175/2008jcli2552.1

Mohtadi, M., Prange, M., & Steinke, S. (2016). Palaeoclimatic insights into forcing and the response of monsoon rainfall. *Nature*, *533*(7602), 191–199. https://doi.org/10.1038/nature17450

Naidu, P. D., Ganeshram, R., Bollasina, M. A., Panmei, C., Nurnberg, D., & Donges, J. F. (2020). Coherent response of the Indian monsoon rainfall to Atlantic multi-decadal variability over the last 2000 years. *Scientific Reports*, *10*(1), 1302. https://doi.org/10.1038/s41598-020-58265-3

NCAR. (2016). Last millennium community experiments, last millennium ensemble (LME). CESM paleoclimate working group at NCAR [Dataset]. Retrieved from https://www.earthsystemgrid.org/dataset/ucar.cgd.ccsm4.cesmLME.html

Ning, L., Chen, K., Liu, J., Liu, Z., Yan, M., Sun, W., et al. (2020). How do volcanic eruptions influence decadal megadroughts over eastern China? *Journal of Climate*, *33*(19), 8195–8207. https://doi.org/10.1175/jcli-d-19-0394.1

Ning, L., Liu, J., & Sun, W. (2017). Influences of volcano eruptions on Asian Summer Monsoon over the last 110 years. *Scientific Reports*, *7*(1), 42626. https://doi.org/10.1038/srep42626

NOAA. (2011). Global Precipitation Climatology Centre (GPCC). Monthly land-surface precipitation from rain-gauges built on GTS-based and historic data [Dataset]. National Oceanic and Atmospheric Administration. Retrieved from https://psl.noaa.gov/data/gridded/data.gpcc.html

NOAA. (2017). NOAA Extended Reconstructed SST V5 (ERSST v5). A global monthly SST analysis [Dataset]. National Oceanic and Atmospheric Administration. Retrieved from https://psl.noaa.gov/data/gridded/data.noaa.ersst.v5.html

Otto-Bliesner, B. L., Fasullo, J., Brady, E. C., Jahn, A., Landrum, L., Stevenson, S., et al. (2016). Climate variability and change since 850 CE: An ensemble approach with the Community Earth System Model. *Bulletin of the American Meteorological Society*, *97*(5), 735–754. https://doi.org/10.1175/bams-d-14-00233.1

PMIP. (2020). The simulations in PMIP3/CMIP5 last millennium experiment. Paleoclimate Modelling Intercomparison Project phase [Dataset]. Retrieved from http://pmip3.lsce.ipsl.fr

Qian, C., & Zhou, T. (2014). Multidecadal variability of North China aridity and its relationship to PDO during 1900–2010. *Journal of Climate*, *27*(3), 1210–1222. https://doi.org/10.1175/jcli-d-13-00235.1

Rustic, G. T., Koutavas, A., Marchitto, T. M., & Linsley, B. K. (2015). Dynamical excitation of the tropical Pacific Ocean and ENSO variability by Little Ice Age cooling. *Science*, *350*(6267), 1537–1541. https://doi.org/10.1126/science.aac9937

Shi, F., Fang, K., Xu, C., Guo, Z., & Borgaonkar, H. P. (2017). Interannual to centennial variability of the South Asian summer monsoon over the past millennium. *Climate Dynamics*, *49*(7–8), 2803–2814. https://doi.org/10.1007/s00382-016-3493-9

Shi, H., Wang, B., Liu, J., & Liu, F. (2019). Decadal–multidecadal variations of Asian summer rainfall from the Little Ice Age to the present. *Journal of Climate*, *32*(22), 7663–7674. https://doi.org/10.1175/jcli-d-18-0743.1

Sinha, A., Kathayat, G., Cheng, H., Breitenbach, S. F., Berkelhammer, M., Mudelsee, M., et al. (2015). Trends and oscillations in the Indian summer monsoon rainfall over the last two millennia. *Nature Communications*, *6*(1), 6309. https://doi.org/10.1038/ncomms7309

Steiger, N. J., Smerdon, J. E., Cook, E. R., & Cook, B. I. (2018). A reconstruction of global hydroclimate and dynamical variables over the Common Era. *Scientific Data*, *5*(1), 180086. https://doi.org/10.1038/sdata.2018.86

Stevenson, S., Brady, E., Fasullo, J., & Otto-Bliesner, B. (2016). “El Niño like” hydroclimate responses to last millennium volcanic eruptions. *Journal of Climate*, *29*(8), 2907–2921. https://doi.org/10.1175/jcli-d-15-0239.1

Stevenson, S., Cole, J., Loope, G., Ault, T., Otto-Bliesner, B., Parsons, L., et al. (2018). Climate variability, volcanic forcing, and last millennium hydroclimate extremes. *Journal of Climate*, *31*(11), 4309–4327. https://doi.org/10.1175/jcli-d-17-0407.1

Sun, C., Liu, L., Li, L.-J., Wang, B., Zhang, C., Liu, Q., & Li, R.-Z. (2018). Uncertainties in simulated El Niño-Southern Oscillation arising from internal climate variability. *Atmospheric Science Letters*, *19*(3), e805. https://doi.org/10.1002/asl.805

Sun, W., Liu, J., Wang, B., Chen, D., & Gao, C. (2022). Pacific multidecadal (50–70 year) variability instigated by volcanic forcing during the Little Ice Age (1250–1850). In *Climate dynamics*. Advance online publication. https://doi.org/10.1007/s00382-021-06127-7

Sun, W., Liu, J., & Wang, Z. (2017). Simulation of centennial-scale drought events over eastern China during the past 1500 years. *Journal of Meteorological Research*, *31*(1), 17–27. https://doi.org/10.1007/s13351-017-6090-x

Sun, W., Wang, B., Liu, J., & Dai, Y. (2022). Recent changes of Pacific decadal variability shaped by greenhouse forcing and internal variability. *Journal of Geophysical Research: Atmospheres*, *127*(8). https://doi.org/10.1029/2021JD035812

Sutton, R. T., & Hodson, D. L. R. (2005). Atlantic Ocean forcing of North American and European summer climate. *Science*, *309*(5731), 115–118. https://doi.org/10.1126/science.1109496

Wang, B., Biasutti, M., Byrne, M. P., Castro, C., Chang, C.-P., Cook, K., et al. (2021). Monsoons climate change assessment. *Bulletin of the American Meteorological Society*, *102*(1), E1–E19. https://doi.org/10.1175/bams-d-19-0335.1

Wang, B., & Ding, Q. (2008). Global monsoon: Dominant mode of annual variation in the tropics. *Dynamics of Atmospheres and Oceans*, *44*(3–4), 165–183. https://doi.org/10.1016/j.dynatmoce.2007.05.002

Wang, B., Jin, C., & Liu, J. (2020). Understanding future change of global monsoons projected by CMIP6 models. *Journal of Climate*, *33*(15), 6471–6489. https://doi.org/10.1175/jcli-d-19-0993.1

Wang, B., Li, J., Cane, M. A., Liu, J., Webster, P. J., Xiang, B., et al. (2018). Toward predicting changes in the land monsoon rainfall a decade in advance. *Journal of Climate*, *31*(7), 2699–2714. https://doi.org/10.1175/jcli-d-17-0521.1

Wang, B., Liu, J., Kim, H. J., Webster, P. J., Yim, S. Y., & Xiang, B. (2013). Northern Hemisphere summer monsoon intensified by mega-El Nino/southern oscillation and Atlantic multidecadal oscillation. *Proceedings of the National Academy of Sciences*, *110*(14), 5347–5352. https://doi.org/10.1073/pnas.1219405110

Wang, J., Yang, B., Ljungqvist, F., Luterbacher, J., Osborn, T., Briffa, K., & Zorita, E. (2017). Internal and external forcing of multidecadal Atlantic climate variability over the past 1,200 years. *Nature Geoscience*, *10*(7), 512–517. https://doi.org/10.1038/ngeo2962

Webster, P. J., Magaña, V. O., Palmer, T. N., Shukla, J., Tomas, R. A., Yanai, M., & Yasunari, T. (1998). Monsoons: Processes, predictability, and the prospects for prediction. *Journal of Geophysical Research*, *103*(C7), 14451–14510. https://doi.org/10.1029/97jc02719

Ying, K., Frederiksen, C. S., Zheng, X., Lou, J., & Zhao, T. (2018). Variability and predictability of decadal mean temperature and precipitation over China in the CCSM4 last millennium simulation. *Climate Dynamics*, *51*(7–8), 2989–3008. https://doi.org/10.1007/s00382-017-4060-8

Zhou, T., Lu, J., Zhang, W., & Chen, Z. (2020). The sources of uncertainty in the projection of global land monsoon precipitation. *Geophysical Research Letters*, *47*(15). https://doi.org/10.1029/2020gl088415

Zuo, M., Zhou, T., & Man, W. (2019). Hydroclimate responses over global monsoon regions following volcanic eruptions at different latitudes. *Journal of Climate*, *32*(14), 4367–4385. https://doi.org/10.1175/jcli-d-18-0707.1

Erratum

In the originally published version of this article, the Author Contributions list contained typographical errors. Deliang Chen should be included under Conceptualization, and Liang Ning and Kefan Chen should be included in Methodology. The errors have been corrected, and this may be considered the authoritative version of record.